Toxicology: Open Access

Elrod et al., Toxicol Open Access 2017, 3:2
DOI: 10.4172/2476-2067.1000124

Research Article OMICS International

Alteration of Cytokine Profiles Inhibits Efficacy of Silver Nanoparticle-based Neutralization of arenaviruses

Nathan Elrod[1], Jeff Brady[2,3], Harold Rathburn[1] and Janice L. Speshock[1*]

[1]*Tarleton State University, Department of Biological Sciences, Stephenville, TX 76402, USA*
[2]*Tarleton State University, Department of Wildlife, Sustainability, and Ecosystem Sciences, Stephenville, TX 76402, USA*
[3]*Texas A&M AgriLife Research and Extension Center, Stephenville, TX 76401, USA*

[*]**Corresponding author:** Janice L. Speshock, Tarleton State University, Department of Biological Sciences, 1333. Washington Street, Box T-0100, Stephenville, TX 76402, USA, Tel: (254) 968-9341; E-mail: speshock@tarleton.edu

Received date: March 27, 2016; **Accepted date:** April 14, 2017; **Published date:** April 19, 2017

Abstract

Background: Arenaviruses are important pathogens that can cause hemorrhagic fever or meningoencephalitis. There is not an effective treatment targeting arenaviruses, which necessitates a search for therapies against this virus family, as well as others. Silver nanoparticles (Ag-NPs) have been shown to have effective antiviral activity in cell culture models against arenaviruses, and therefore it was hypothesized that they may make an effective therapeutic against viral meningitis. However, the silver nanoparticles interfered with normal cytokine profiles produced in response to the virus infection, which led to exacerbated pathology.

Methods: Mice were infected with Tacaribe virus, a mouse-adapted arenavirus that causes lethal encephalitis. The virus was left untreated or treated with 10 nm Ag-NPs, which were demonstrated previously to inhibit virus replication in cell culture. Virus replication, brain pathology, and cytokine profiles (pro-inflammatory interleukins and type I interferons), as well as over morbidity and mortality were assessed in the mice with and without treatment.

Results: Although the viral loads appeared to be reduced in the Ag-NP treated mice, mortality was observed in all virus-infected animals, regardless of whether or not they received nanoparticle therapy. The Ag-NP treatments also impacted the innate immune response against the virus infection and unregulated the production of interleukin-1 beta, which likely contributed to the observed mortality in the mice.

Conclusions: This study confirms why it is important to assess promising *in vitro* results using *in vivo* models. Biological barriers can impact the efficacy of therapeutics in mammals. Although Ag-NPs may still have success as an antiviral therapeutic in other areas of the body that are less constricted, in sensitive areas such as the brain, the nanoparticles can cause very adverse reactions.

Keywords: Silver nanoparticles; Immunotoxicology; Inflammation; Interferons; Arenavirus; Tacaribe virus

Introduction

The *Arenaviridae* family of 18 species of viruses is divided into New World and Old World clades [1]. These viruses have an ambisense RNA genome with two structural segments, the S segment and the L segment, each encoding viral proteins [1]. The New World, or Tacaribe Serocomplex, clade consists of Tacaribe Virus (TCRV), as well as the hemorrhagic fever viruses Junin and Machupo [1,2]. At an amino acid level TCRV is a 67-78% match to the highly pathogenic Junin in the 4 main viral proteins (NP, GPC, L, and Z) [3]. TCRV is unique from other arenaviruses in that it fails to suppress host type I and II interferon (IFN), and consequently, does not cause viral hemorrhagic fever in humans making it safe for study at the biosafety level 2 (BSL-2) [4,5]. TCRV is also unusual compared to other members of *Arenaviridae* as it has been isolated in bats as opposed to the strict use of rodent hosts in the other arenaviruses in its clade, however it can be mouse-adapted quite easily for use in rodent models [6]. In BALB/c mice of all ages inoculated intra-cranially (IC), following serial passage, TCRV can manifest clinical symptoms (ruffled fur, hind limb paralysis, lethargy) in 9 to 11 days followed by death 1 to 3 days after symptoms manifest [7,8]. Newborn BALB/c mice and immunocompromised mice lacking IFN-α/β and IFN-γ receptors inoculated intra-peritoneally (IP) also showed the same clinical symptoms followed by death in the same time-frame [9,10]. Mouse-adaptation of TCRV causes mortality by lethal meningoencephalitis, or lesions in both the meninges and brain tissue caused by inflammation, *via* over-activation of the cellular immune response, which is more similar to the pathology observed with the Old World human arenavirus, Lymphocytic Choriomeningitis Virus (LCMV) [7-11]. There are a lack of therapies and preventative measures to combat hemorrhagic fever and meningitis infections caused by arenaviruses [12]. An effective treatment to arenavirus infection would require the combination of an agent that will limit both virus replication and the proinflammatory cellular response, which contributes to the swelling observed in viral meningoencephalitis [13].

Nanomaterials have been shown to have numerous physical, biological, and pharmaceutical properties, including antiviral [14]. Silver nanoparticles (Ag-NPs) in the 10 to 20 nm size range, have been shown to prevent viral replication of Human Immunodeficiency Virus type 1 [15], Monkeypox virus [16], adenovirus serotype 3 [17], and TCRV using cell culture models [18]. It is hypothesized that the Ag-NPs inhibit viral infection by binding to the viral glycoproteins to

prevent association of the virion with the host cell receptor, or as in the case of TCRV, to stimulate the uptake of an inert virus particle [15-18]. TCRV was shown to associate with the Ag-NPs, but instead of blocking binding, as observed with most viruses, the association of Ag-NPs and TCRV increased the binding efficiency and uptake of the virions into Vero cells, but the virus did not replicate once it was internalized, thus demonstrating virus inactivation [18]. It was therefore hypothesized that similar inhibitory effects could be demonstrated using mouse-adapted TCRV with Ag-NP treatment in Balb/c mice. Juvenile mice were inoculated IC with TCRV treated with Ag-NPs, and the resulting morbidity and mortality of the virus was observed in Ag-NP and mock-treated infections.

Materials and Methods

Mouse adaptation of TCRV

All procedures were performed under an approved protocol by the Tarleton State University Institutional Animal Care and Usage Committee to ensure laboratory animal health and safety. The virus was mouse adapted following three serial IC passages in 7 week old ICR (CD-1) mice (Harlan Laboratories, Indianapolis, IN) to increase virulence using a modified protocol [8]. Briefly, thirty microliters of TCRV (VR-1556; ATCC, Manassas, VA) was given IC to 3 mice. Mice were observed daily and were sacrificed *via* lethal injection of sodium pentobarbital (150 µL IP) when mice demonstrated clinical symptoms of severe inactivity or inappetence, or had lost more than 25% of their initial body weight, which occurred in two of the three mice at day 6 post-infection. Those two mice were sacrificed and the brain tissues were harvested and homogenized in 1 ml of TNE buffer (0.01 M Tris-HCl, 0.15 M NaCl, 1 mM EDTA, buffered at pH 7.4). The homogenized brains from the 2 mice showing signs of illness were combined in equal 100 µL proportions to create a total volume of 200 µL of homogenate which was combined with 200 µL of Fetal Bovine Serum (FBS; Atlanta Biologicals, Norcross, GA) and 600 µL of TNE to create serial passage 1 (TCRVp1). This process was repeated with two additional serial passages into the brain to generate a stock that was lethal to 100% of mice (TCRVp3), which was determined using a viral plaque assay to be 6.5 x 10^5 plaque forming units (pfu)/mL. This inoculum was stored at -80°C until further experimentation.

Viral attenuation with Ag-NPs

Biopure silver nanospheres at a diameter of 10 ± 2 nm were obtained from nanoComposix Inc (San Diego, CA). The nanoparticles were synthesized with a 0.01% polyvinylpyrrolidone (PVP) coating to increase biological stability and decrease toxicity [19]. PVP coating is used to keep the nanoparticles from agglomeration during manufacture and reduces cytotoxic effects *in vitro* [19,20]. The ability of Ag-NPs to neutralize TCRV was performed in a similar experimental design as an *in vitro* neutralization assay in Vero cells [18]. The lethal dose at 50% (LD_{50}) for the virus *via* IC inoculation was determined to be 280 pfu/mL, therefore a 1000-fold dilution of TCRVp3 (650 pfu/mL) was used to assess Ag-NP neutralization. This concentration of TCRV was incubated with 50 µg/mL of Ag-NP, 25 µL of 0.01% PVP, which reflected the amount of PVP in the Ag-NP sample at 50 µg/mL, or 25 µL TNE. These viral suspensions were then incubated at room temperature in a rotating mixer for 1 hour to allow for interaction. The dosage of 50 µg/mL nanoparticle was used as it had been determined to have a completely inhibitory effect on Tacaribe virus in Vero cells [18].

These attenuated preparations were then given at 30 µL IC to groups of ICR mice (n=4) at 7 weeks old. Morbidity and mortality between the Ag-NP and control groups were recorded for comparison. In addition, brain tissue was excised post mortem for RNA extraction and histopathological examination. One mouse per group's brain was preserved in 4% paraformaldehyde and sent for histological processing and slide preparation with hematoxylin and eosin staining. The remaining mice brains were homogenized in 1 mL TNE each and 50µL of homogenate was used for mRNA extraction.

Messenger RNA Extraction

RNA was extracted from the mouse brains using 50 µL of brain homogenate and the GET Total RNA kit, with optional DNase treatment, from G-biosciences (St. Louis, MO) as per the manufacturer's instructions. The mRNA was quantified using the Quant-iT Ribogreen RNA assay kit (ThermoFisher Scientific, Waltham, MA) in a BioTek Flx800 multiwell fluorimeter (Winooski, VT). All RNA samples were normalized to 500 nanograms (ng) of RNA.

Quantitative reverse transcriptase polymerase chain reaction (qRT-PCR)

One microliter of each RNA sample was added to 2.5 µL of Sybr green, 1 µL DNase/RNase-free water, and 0.5 µL of reverse transcriptase from the qScript One-Step SYBR Green qRT-PCR kit (Quanta Biosciences, Beverly, MA) and 0.5 µL of primer mix (0.2 µM of each primer). Each RNA sample was prepared in triplicate with each primer set listed in Table 1 and loaded into a 384-well PCR plate for analysis in the Roche 480 Light Cycler (Basel, Switzerland) to determine the threshold cycle of each sample. An initial 10 minute incubation at 50°C allowed for the conversion of the RNA to complementary DNA using reverse transcriptase, which was then followed by the following cycles for DNA amplification: 1 minute denature at 95°C; 45 cycles of 10 seconds at 95°C, 30 seconds at 60°C with a quantification fluorescence read, and 30 seconds at 72°C; followed by a melt curve of 10 seconds at 95°C, 30 seconds at 40°C with continuous fluorescence readings to 95°C; and a final cool down to 40°C. The threshold cycles were used to determine the fold change using the delta-delta CT method [21].

Gene	Forward Primer	Reverse Primer
TCRV S [18]	TGTGTTGGCTGGCAGAT	AGGAGAGTGAACAAAGACAT
IFNα [22]	GGACTTTGGATTCCCGCAGGAGAAG	GCTGCATCAGACAGCCTTGCAGGTC
IFNβ [22]	AACCTCACCTACAGGGCGGACTTCA	TCCCACGTCAATCTTTCCTCTTGCTT
IL-1β [23]	CAACCAACAAGTGATATTCTCCATG	GATCCACAGTGTGGACGTGCA
IL-6 [23]	GAGGATACCACTCCCAACAGACC	AAGTGCATCATCGTTGTTCATACA
TNFα [23]	CATCTTCTCAAAATTCGAGTGACAA	TGGGCGTAGACAAGGTACAACCC
L19 [24]	ATGAGTATGCTCAGGCTACAG	TGACGGGAGTTGGCATTG

Table 1: Primer sequences for qRT-PCR.

Histology

Formalin-fixed brains were shipped to Tarleton State University Department of Medical Laboratory Sciences (Fort Worth, TX) for histological processing and slide preparation. The slides were stained with hematoxylin and eosin for viewing of histopathology. The slides were viewed on a Zeiss Jenalumar Contrast Microscope (Oberkochen, Germany) and imaged using a WESCO 291CU digital camera (Pittsburgh, PA).

Statistical analysis

All qRT-PCR analyses were compared between control and treatment groups using a one-way Analysis of Variance (ANOVA) with significance determination at $p< 0.05$. Histopathic effect was reported by visual observation.

Results

Ag-NP neutralization of TCRV

Although mice that received an inoculation of Ag-NP-treated TCRV lived longer than mice that received a mock attenuation of TCRV (12 days versus 6 days), only one of the Ag-NP treated mice survived the exposure Table 2. This compared to 0 mice in the mock-treatment (TNE) or PVP treatment Table 2.

Attenuation Treatment	Number of mice that survived (n=4)
TNE+TCRV	0
PVP+TCRV	0
Ag-NP+TCRV	1

Table 2: Survivability assessment of TCRV-infected mice following attenuation treatments (n=4).

TCRV replication following Ag-NP attenuation

Replication of TCRV was compared using qRT-PCR analysis with primers specific for the S segment of the virus Table 1. A significant reduction of S segment RNA replication was observed when the TCRV was pre-incubated with Ag-NPs as compared with incubation with either TNE or PVP, which indicated that the Ag-NPs were capable of inhibiting virus replication Figure 1. Although there was a reduction in TCRV replication in the Ag-NP-treated TCRV infections, there were no significant changes in pfu/ml from the brains of mice infected with TCRV that were treated with TNE, PVP, or Ag-NP. All three treatment groups produced an average of approximately 70 pfu/ml of brain homogenate (data not shown). This suggests that the Ag-NPs themselves may be inducing cytotoxicity in the cell culture used for the plaque assays.

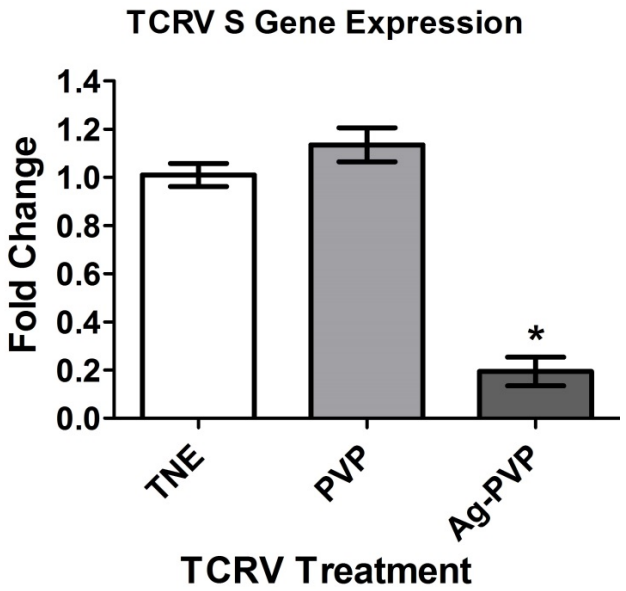

Figure 1: TCRV S segment gene expression analysis. Fold change expression of the S segment of the viral genome was normalized to the TNE-treated TCRV mouse brains and compared to brains from PVP or PVP-coated Ag-NP treatment of TCRV (n=4). *indicates significant reduction ($p<0.05$).

Histopathological examination of TCRV-infected mice

Representative images of the brains of uninfected mice or TCRV-infected mice following pre-incubation of the virus with either TNE or Ag-NP depicted noticeable histopathological changes compared to the control mice (no virus infection) Figures 2 and 3. Serial frontal sections of brain specimens were examined microscopically. Anterior transections including regions of the thalamus and cerebral cortex were examined as well as the meningeal layer surrounding the brain. There were no observable changes in the meninges of any treatment group from the control (data not shown). However, there was a noticeable breakdown in the architecture of the thalamus of the TNE/TCRV-infected mice Figures 2A and 2B and cytopathic effect observed in the cerebral cortex of these mice Figure 2E. The thalamus remained intact for the mice treated with Ag-NP/TCRV Figure 2C, but large vacuoles formed in the cerebral cortex Figure 2F that were not evident in either of the other mice Figures 2A-F. A large blood vessel in the cerebellum depicted an increase in erythrocyte infiltration, suggesting hemorrhaging, in the TNE/TCRV-treated mice over control, and the AG-NP/TCRV-treated mice displayed not only an erythrocyte infiltration, but also leukocyte and lymphocyte migration, which could be causing immunopathology Figures 3A-F.

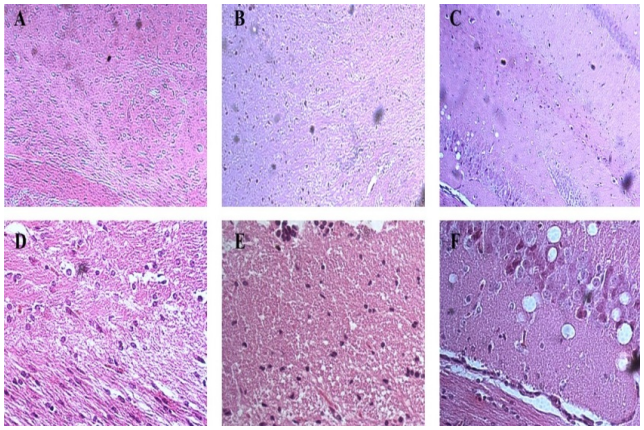

Figure 2: Histological examination of brains from TCRV-infected mice. Frontal cross sections from the center of the brain including the thalamus-cerebral cortex border from the brains of mice that were infected with TCRV that had been pre-treated with TNE (a and d), PVP (b and e), or Ag-NPs (c and f). The top 3 images (a-c) are at 6.3x magnification and the bottom 3 images (d-f) represent the lower left quadrant of the 6.3x image magnified to 50x.

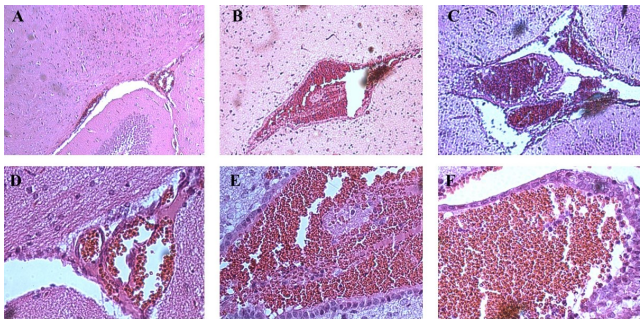

Figure 3: Histological examination of brain vasculature from TCRV-infected mice. Frontal cross sections from the center of the brain including a blood vessel from the cerebellum of brains of mice that were infected with TCRV that had been pre-treated with TNE (a and d), PVP (b and e), or Ag-NPs (c and f). The top 3 images (a-c) are at 6.3x magnification and the bottom 3 images (d-f) represent the lower left quadrant of the 6.3x image magnified to 50x.

Immune responses in the brains of TCRV-infected mice

Since there was a reduction in TCRV replication following Ag-NP treatment, but an increase in observable histopathology, it was hypothesized that the immune system was contributing to the pathology. Type I interferon (IFN) responses were assessed since they have been shown to contribute greatly to the recovery from arenavirus infections. A slight decline in IFN beta and a significant reduction in IFN alpha were observed following Ag-NP treatment Figure 4, which should have led to an increase in virus replication, not a decrease, suggesting further that the Ag-NPs themselves might be contributing to the pathology and mortality observed, by suppressing immune function. It was also hypothesized that the Ag-NPs were stimulating an inflammatory response, which would cause swelling of the brain, and thereby significant morbidity and mortality. Therefore the gene expression changes were assessed for the pro-inflammatory cytokines interleukin-1 beta (IL-1β), interleukin-6 (IL-6), and tumor necrosis factor alpha (TNF-α). There were no differences observed in the expression of IL-1β or TNF-α with any of the treatment groups compared to control, and the IL-6 TCRV infection with Ag-NP treatment actually had a reduction in expression Figure 5. These data indicate that there was no induction of inflammation contributing to the pathology of the mice brains, and that the Ag-NPs may suppress immune response in infected animals.

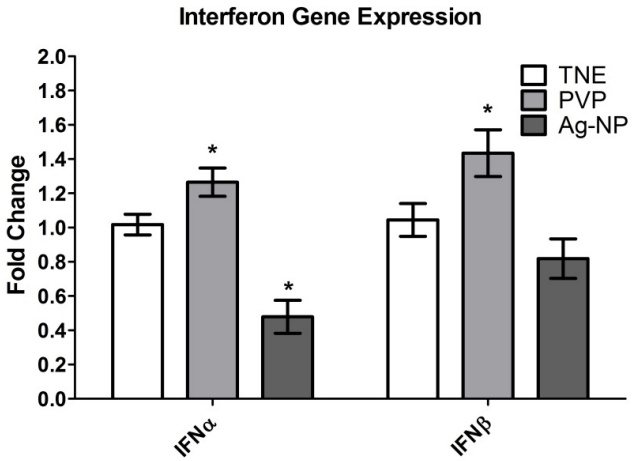

Figure 4: Type I interferon gene expression analysis. Fold change expression of the host type I interferons (alpha and beta) were normalized to the TNE-treated TCRV mouse brains and compared to brains from PVP or PVP-coated Ag-NP treatment of TCRV (n=4). *indicates significant change in gene expression ($p<0.05$).

Discussion

Attenuation with silver nanoparticles did impact the amount of innate immune response by the host Figures 4 and 5, which likely contributed to the observed pathology since there was also a reduction in TCRV S segment expression, following pre-incubation with Ag-NPs, compared to controls Figure 1. The inactivation of the virus was not sufficient to prevent death in the majority of the mice tested Table 1, which leads one to hypothesize that the Ag-NPs may be causing cell death of the neurons in addition to the virus through a direct or indirect (inflammation) mechanism. An *in vitro* cell culture model did not demonstrate any discernable cell death from the virus-nanoparticle agglomerate [18], but the cells used for this study were kidney cells, which tend to be more stable than neurons [18,20]. Also, the *in vitro* study utilized Ag-NPs that were uncoated or polysaccharide-coated, and the Biopure PVP coating may have interfered with the TCRV interaction with silver. The first attempt *in vivo* was using the uncoated 10 nm Ag-NPs from the same manufacturer as the cell culture trials, but there was no decline in mortality and a great deal of inflammation was observed (data not shown). Therefore a more biocompatible polymer coating was selected for the Ag-NPs for the *in vivo* study, to decrease side-effects from the nanoparticle. These PVP-coated Ag-NPs do exhibit some mild *in vivo* toxicity and inflammation [25], but did not cause mortality alone in an open system [25]. However, the sensitivity of neurons to external stimuli and the enclosed nature of the

mouse brain may have exacerbated the toxicity of the nanoparticles. Mouse neuroblastoma cells have been shown to be much more sensitive to nanoparticle toxicity than African Green Monkey kidney cells (Vero cells) using cell culture toxicity assays [18,20]. In previous studies of TCRV, it was demonstrated that the Purkinje cells of the cerebellum appear to be the major targets of the virus, which may be more vulnerable to increases in inflammation and decreases in the anti-viral protection of the interferons [8]. The histology obtained from this study showed most histological changes around the regions of the thalamus and the cerebellum, confirming this target area for the virus. Since more histopathological effects occurred in the nanoparticle-treated virus infection, it is possible that the virus is targeting the Purkinje cells allowing for increased uptake of the Ag-NPs, which in turn are causing cytotoxicity.

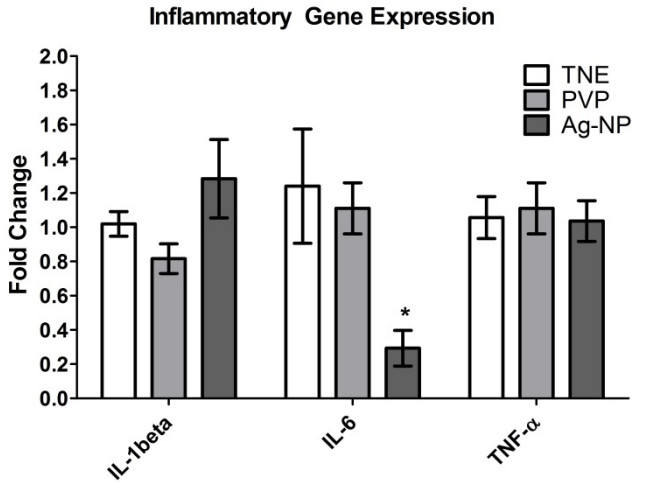

Figure 5: Inflammatory gene expression analysis. Fold change expression of the pro-inflammatory cytokine genes were normalized to the TNE-treated TCRV mouse brains and compared to brains from PVP or PVP-coated Ag-NP treatment of TCRV (n=4). *indicates significant reduction ($p<0.05$).

This study illustrates the potential conflict in the results between an *in vitro* study, where the virus was completely inactivated, and an *in vivo* study, where there is still mortality from the virus infection, although it is hypothesized that the Ag-NPs are causing the mortality. Cell culture models lack the diversity of cell populations and complexity of living organisms, and therefore can be misleading at times. Neurons are generally not utilized *in vitro* for virus studies due to their known instability against external stimuli [19]. Either the replication-deficient virions, the Ag-NPs, or both, are capable of destroying these sensitive cells in an *in vivo* model of infection. Since Xiang et al. demonstrated efficacy of Ag-NPs *in vivo* against influenza virus [26], there still is the possibility of using Ag-NPs as a broad-spectrum antiviral agent, but anatomical location of treatment may need to be considered prior to use, especially in more sensitive areas like the brain.

Declarations

Animal Ethics Approval

All procedures were performed under an approved protocol (AUP_Speshock_2014) by the Tarleton State University Institutional Animal Care and Usage Committee to ensure laboratory animal health and safety. Animals were housed according to guidelines outlined in an approved standard operating procedures (SOP_0026) document.

Competing Interests

The authors have no competing interests to declare.

Acknowledgements

This project was funded through Tarleton State University's Office of Student Research and Creative Activities through a Student Research Grant awarded to Mr. Elrod. There was no external funding source for this research. We would like to thank Dr. Brooke Dubansky from Tarleton State University Medical Laboratory Sciences for histological processing and staining.

References

1. Buchmeier MJ, Bowen MD, Peters CJ (2013) *Arenaviridae*. Fields Virology. 6thedn Lippincott, Williams & Wilkins, Philadelphia, pp: 1283-1303.
2. Charrel RN, de Lamballerie X (2003) Arenaviruses other than Lassa virus. Antiviral Res 57: 89-100.
3. Bolken TC, Laquerre S, Zhang Y, Bailey TR, Pevear DC, et al. (2006) Identification and characterization of potent small molecule inhibitor of hemorrhagic fever New World arenaviruses. Antiviral Res 69: 86-97.
4. Bray M (2005) Pathogenesis of viral hemorrhagic fever. Curr Opin Immunol 17: 399-403.
5. Martinez-Sobrido L, Giannakas P, Cubitt B, García-Sastre A, Carlos de la Torre J (2007) Differential inhibition of type I interferon induction by arenavirus nucleoproteins. J Virol 81: 12696-12703.
6. Downs WG, Anderson CR, Spence L, Aitken TH, Greenhall AH (1963) Tacaribe virus, a new agent isolated from artibeus bats and mosquitoes in Trinidad, West Indies. Am J Trop Med Hyg 12: 640-646.
7. Borden EC, Nathanson N (1974) Tacaribe Virus-Infection of Mouse - Immunopathologic Disease Model. Laboratory Investigation 30: 465-473.
8. Rosato RR, Elwell MR, Eddy GA (1978) Virulence alterations of tacaribe virus infection in adult mice: lethal model for encephalitis. Arch Virol 58: 137-147.
9. Gowen BB, Wong MH, Larson D, Ye W, Jung KH, et al. (2010) Development of a new Tacaribe arenavirus infection model and its use to explore antiviral activity of a novel aristeromycin analog. Plos One 5: 11.
10. Borden EC, Murphy FA, Nathanson N, Monath TPC (1971) Effect of antilymphocyte serum on Tacaribe virus infection in infant mice. Infect Immun 3: 466–471.
11. Shresta S, Sharar KL, Prigozhin DM, Beatty PR, Harris E (2006) Murine model for dengue virus-induced lethal disease with increased vascular permeability. J Virol 80: 10208-10217.
12. Leyssen P, De Clercq E, Neyts J (2008) Molecular strategies to inhibit the replication of RNA viruses. Antiviral Res 78: 9-25.
13. Sefing EJ, Wong MH, Larson DP, Hurst BL, Van Wettere AJ, et al. (2010) Vascular leak ensues a vigorous proinflammatory cytokine response to Tacaribe arenavirus infection in AG129 mice. Virology Journal 10: 221.
14. Sondi I, Salopek-Sondi B (2007) Silver nanoparticles as antimicrobial agent: a case study on E. coli as a model for Gram-negative bacteria. J Colloid Interface Sci 275: 177-182.

15. Elechiguerra JL, Burt JL, Morones JR, Camacho-Bragado A, Gao X, et al. (2005) Interaction of silver nanoparticles with HIV-1. J Nanobiotechnology 3: 6.
16. Rogers JV, Parkinson CV, Choi YW, Speshock JL, Hussain SM (2008) A preliminary assessment of silver nanoparticle inhibition of monkeypox virus plaque formation. Nanoscale Res Lett 3: 129-133.
17. Chen N, Zheng Y, Yin J, Li X, Zheng C (2013) Inhibitory effects of silver nanoparticles against adenovirus type 3 in vitro. J Virol Methods 193: 470-477.
18. Speshock JL, Murdock RC, Braydich-Stolle LK, Schrand AM, Hussain SM (2013) Interaction of silver nanoparticles with Tacaribe virus. J Nanobiotechnology 8: 19.
19. Kittler S, Greulich C, Gebauer JS, Diendorf J, Treuel L, et al. (2010) The influence of proteins on the dispersibility and cell-biological activity of silver nanoparticles. J Mater Chem 20: 512-518.
20. Schrand AM, Braydich-Stolle LK, Schlager JJ, Dai L, Hussain SM (2008) Can silver nanoparticles be useful as potential biological labels? Nanotechnol 19: 235104.
21. Livak KJ, Schittgen TD (2001) Analysis of relative gene expression data using real-time quantitative PCR and the 2-ΔΔCT method. Methods 25: 402–408.
22. Liu G, Friggeri A, Yang YP, Park YJ, Tsuruta Y, et al. (2009) miR-147, a microRNA that is induced upon Toll-like receptor stimulation, regulates murine macrophage inflammatory responses. PNAS 106: 15819-15824.
23. Overbergh L, Giulietti A, Valckx D, Decallonne R, Bouillon R, et al. (2003) The use of real-time reverse transcriptase PCR for the quantification of cytokine gene expression. J Biomol Tech 14: 33-43.
24. Speshock JL, Doyon-Reale N, Rabah R, Neely MN, Roberts PC (2007) Filamentous influenza A virus infection predisposes mice to fatal septicemia following superinfection with Streptococcus pneumoniae serotype 3. Infect Immun 75: 3102-3111.
25. Speshock JL, Elrod N, Sadoski DK, Maurer E, Braydich-Stolle LK, et al. (2016) Differential organ toxicity in the adult zebra fish following exposre to acute sub-lethal dose of 10 nm silver nanoparticles. Frontiers in Nanosci and Nanotechnol 2: 114-120.
26. Xiang D, Zheng Y, Duan W, Li X, Yin J, et al. (2013) Inhibition of A/Human/Hubei/3/2005 (H3N2) influenza virus infection by silver nanoparticles in vitro and in vivo. Int J Nanomed 8: 4103-4114.